



Study on the correlation between energy spectrum computed tomography imaging and the pathological characteristics and prognosis of cervical cancer

Libo Pan¹, Xia Jia¹, Xuwu Zhao¹, Bei Zhang¹, Shusheng Wang¹, Tao Fan¹, Min Zhou², Yuan Yuan², Guoqing Wang², Longmei Xue¹

¹Department of Computed Tomography, Shaanxi Provincial Cancer Hospital, Xi'an, China; ²Department of Female Tumor, Shaanxi Provincial Cancer Hospital, Xi'an, China

Contributions: (I) Conception and design: L Pan, X Jia; (II) Administrative support: None; (III) Provision of study materials or patients: S Wang, T Fan; (IV) Collection and assembly of data: X Zhao, M Zhou; (V) Data analysis and interpretation: Y Yuan, L Xue; (VI) Manuscript writing: All authors; (VII) Final approval of manuscript: All authors.

Correspondence to: Longmei Xue. Department of Computed Tomography, Shaanxi Provincial Cancer Hospital, 309 Yanta West Road, Xi'an 710061, China. Email: 18066621992@189.cn.

Background: The purpose of this study is to investigate the correlation between energy spectrum computed tomography (CT) imaging and the pathological characteristics and prognosis of cervical cancer.

Methods: All participants underwent energy spectrum CT plain scan and enhanced scan of the cervix, uterine body, and common iliac vein. The correlation between the slope of energy spectrum attenuation curve and pathological characteristics and curative effect was analyzed, and the receiver operating characteristic (ROC) curve of the slope of energy spectrum attenuation curve to distinguish some pathological characteristics and curative effect was constructed.

Results: The energy spectrum curves of cervix, uterine body, and common iliac vein all showed a downward trend. The slope of cervix energy spectrum curve showed a significant difference in different differentiation degree ($P < 0.05$), and the slope of energy spectrum curve showed an upward trend. The slope of energy spectrum curve of common iliac vein was significantly different between high and low cell proliferation antigen marker (Ki67) ($P < 0.05$), and the slope of Ki67 high expression was higher than that of Ki67 low expression. Treatment was effective in 17 participants and ineffective in 11. After treatment, the energy spectrum curve slope of cervix and energy spectrum curve slope of common iliac vein in the effective group were significantly increased compared with before treatment ($P < 0.05$), and the energy spectrum curve slope of cervix in the ineffective group was increased compared with before treatment, but the difference was not significant ($P > 0.05$). The area under the curve (AUC) of distinguishing Ki67 expression of energy spectrum curve slope of common iliac vein was 0.7008, sensitivity was 66.67%, and specificity was 62.34%. The AUC of distinguishing the curative effect of cervical energy spectrum curve slope was 0.6131, sensitivity was 56.25%, and specificity was 59.09%. The AUC of distinguishing the curative effect of energy spectrum curve slope of common iliac vein was 0.6563, sensitivity was 60.42%, and specificity was 58.33%.

Conclusions: The energy spectrum curve slope has potential value in the prediction of certain specific pathological types of cervical cancer and the evaluation of curative effect.

Keywords: Energy spectrum CT imaging; cervical cancer; pathological features; evaluation of curative effect

Submitted Jun 25, 2021. Accepted for publication Aug 26, 2021.

doi: 10.21037/tcr-21-1320

View this article at: <https://dx.doi.org/10.21037/tcr-21-1320>

Introduction

Cervical cancer is one of the most common malignant tumors in gynecology. In China, the incidence of cervical cancer is second only to breast cancer and has shown a younger and rising trend in recent years (1,2). Cervical cancer is mainly associated with human papilloma virus (HPV) infection, excessive childbirth (or abortion), and other factors. Patients may experience symptoms such as vaginal bleeding, increased vaginal discharge, frequent urination, and urinary urgency. There are no obvious clinical symptoms in the early stage. Once obvious symptoms appear, most patients are diagnosed as advanced stage and have already missed their optimal treatment window. Therefore, early diagnosis and timely evaluation of curative effect are key to the treatment of cervical cancer. At present, imaging methods are most commonly used in clinical practice to provide effective a basis for the diagnosis and treatment of cervical cancer.

Computed tomography (CT) is an effective imaging method for the diagnosis of cervical cancer, and with the upgrading of CT equipment and the innovation of image post-processing technology, it can not only accurately reflect the morphological characteristics of the primary site of cervical cancer and distant lymph node metastasis, but also reflect the pathophysiological characteristics of cervical cancer lesions. Energy spectrum CT is a relatively new core imaging technology. It uses fast kV switching technology to obtain monochromatic images of tissues at different energies (3-5), and can obtain energy spectrum attenuation curves through material separation technology, allowing the calculation of CT values, which expanded the functions of traditional CT (6), and provide more clinical indicators and analysis tools. At present, energy spectrum CT has made good progress in the diagnosis of tumors, and the accuracy and specificity of the diagnosis and staging of some tumors are getting continually increasing. However, few studies have reported the application of energy spectrum CT imaging technology in cervical cancer. Therefore, 28 patients with cervical cancer in our hospital were included in this study. All patients received plain CT scan and energy spectrum enhanced CT scan of the cervix, uterine body, and common iliac vein. The correlation between the energy spectrum attenuation curve slope and pathological characteristics and curative effect was analyzed, and the receiver operating characteristic (ROC) curve of the energy spectrum attenuation curve slope to distinguish part of pathological characteristics and curative effect

was constructed, in order to explore the application value of energy spectrum CT imaging in cervical cancer. We present the following article in accordance with the STARD reporting checklist (available at <https://dx.doi.org/10.21037/tcr-21-1320>).

Methods

General information

From January 2018 to January 2020, 28 patients with cervical cancer admitted to our hospital were selected as the research cohort. The inclusion criteria were as follows: (I) aged 18–70 years old; (II) patients who underwent CT plain scan + energy spectrum enhanced CT scan (scan range included at least below the diaphragm to the pubic symphysis); (III) cervical cancer discovered for the first time without any anti-tumor treatment (such as radiotherapy and chemotherapy); (IV) patients diagnosed with cervical cancer by pathological biopsy and imaging examination. The exclusion criteria were as follows: (I) pregnant and lactating women; (II) the scan did not meet the standard, the patient's examination preparation was not perfect, or the contrast media injection factors did not meet the diagnostic criteria; (III) patients who had not signed the informed consent. The study was conducted in accordance with the Declaration of Helsinki (as revised in 2013). All participants provided written informed consent, and this experiment was approved by the Ethics Committee of Shaanxi Provincial Cancer Hospital (202061684).

Examination method

The patient assumed a supine position, scanning direction was head-first, breathing training was performed before scanning, and abdomen and pelvic energy spectrum enhanced scanning was performed. The scanning parameters were set to: 100 kV/Sn140 kV, automatic default mAs system, 60 mL of non-ionic contrast agent ioversol (300 mgI/mL) was injected through the elbow vein with a high-pressure syringe, the injection flow rate was 3 mL/s, and then 80 mL of normal saline was injected at the same flow rate. The scanning was performed after the arterial phase was delayed for 30 s and the venous phase was delayed for 65 s. The layer with maximum diameter of the tumor was selected as the perfusion center layer, scanning range was 50 mm, and the scanning layer thickness was 5 mm. Scanning results were transmitted to the workstation,

and a perfusion scanning software package was used for data analysis. The “single energy +” mode was selected. Image processing and analysis were performed by 2 experienced radiologists, and the region of interest (ROI) of the lesion was drawn. After image analysis and processing, the processing software was used to automatically obtain the single-energy CT values corresponding to 40–140 keV, and a total of 110 single-energy CT values of 40–140 keV (interval of 10 keV) were recorded for statistical analysis. The energy spectrum attenuation curve was plotted with

keV as the abscissa and CT value as the ordinate, and the energy spectrum curve slope between 40 and 100 keV was selected for statistical analysis.

Statistical analysis

The software SPSS 22.0 (IBM Corp., Chicago, IL, USA) was used for statistical analysis. Measurement data were expressed as mean \pm standard deviation (SD), and compared and analyzed by *t*-test. An ROC curve was used to draw the energy spectrum curve to distinguish pathological features and efficacy. A *P* value <0.05 was considered statistically significant.

Results

Baseline information

The average age of the 28 participants was 49.07 ± 11.66 years, and the average body mass index (BMI) was 23.85 ± 4.17 kg/m². The remaining baseline information is shown in *Table 1*. The test process is shown in *Figure 1*.

CT signs

The CT signs illustrated in *Figure 2* show that the cervix was enlarged, with a diameter of more than 3.5 cm, asymmetrical contours, and irregular lateral margin. In the venous phase of the enhanced scan, there were irregular masses and low-density masses with lower density than normal cervical tissue, suggesting necrosis within the tumor or lesions, and slightly larger lymph nodes beside the external iliac vessels.

Table 1 Baseline information

Item	Subtypes	n (%)
Age	>49 years	13 (46.43)
	≤ 49 years	15 (53.57)
BMI	>23	11 (39.29)
	≤ 23	17 (60.71)
Pathological type	Squamous cell carcinoma	20 (71.43)
	Adenocarcinoma	5 (17.86)
	Squamous cell carcinoma with adenoid differentiation	3 (10.71)
Differentiated degree	Low differentiation	2 (7.14)
	Middle differentiation	12 (42.86)
	High differentiation	4 (14.29)
	Missing	8 (28.57)
Ki67	High expression	16 (57.14)
	Low expression	12 (42.86)

BMI, body mass index; Ki67, cell proliferation antigen marker.

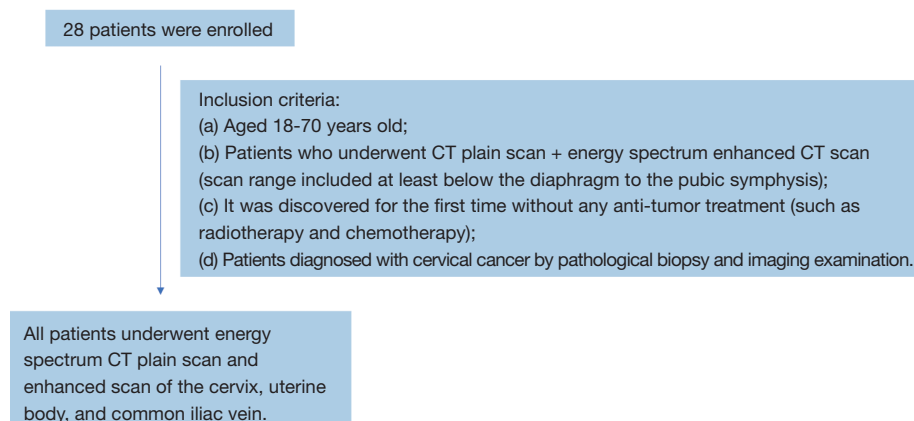


Figure 1 Flow of participant involvement. CT, computed tomography.

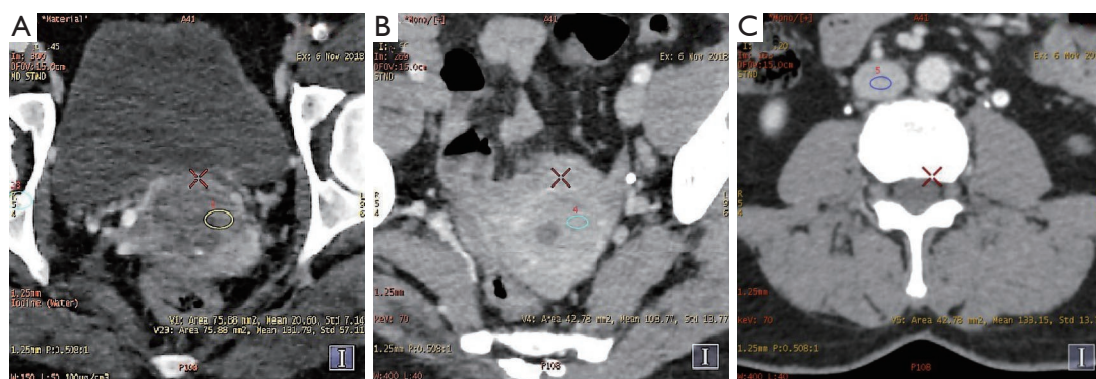


Figure 2 CT images. (A) Cervix (yellow circle); (B) uterine body (blue circle); (C) common iliac vein (purple circle). CT, computed tomography.

The relationship between CT value and pathological features

In the venous phase of energy spectrum enhanced CT scan between 40 and 50 keV, the CT value of cervical lesions with low differentiation degree was significantly higher than that with medium or high differentiation degree ($P < 0.05$), and the CT value with high expression of cell proliferation antigen marker (Ki67) was significantly higher than that with low expression of Ki67 ($P < 0.05$). The CT value of squamous cell carcinoma was significantly lower than that of adenocarcinoma in enhanced scanning of uterine body ($P < 0.05$). At 60–140 keV, there was no significant difference in CT value in enhanced scanning of the cervix and uterine body ($P > 0.05$). At 40 keV, the CT value of squamous cell carcinoma was significantly lower than that of adenocarcinoma in the enhanced scanning of common iliac vein ($P < 0.05$), and the CT value with low differentiation degree was significantly higher than that with medium or high differentiation degree ($P < 0.05$). At 50–140 keV, there was no significant difference in CT value in the enhanced scanning of the common iliac vein ($P > 0.05$) (Tables 2–4).

Relationship between the energy spectrum curve slope and the pathological characteristics

The energy spectrum curves of cervix, uterine body, and common iliac vein all showed a downward trend. The energy spectrum curve slope of uterine body and cervix showed significant difference in different differentiation degree ($P < 0.05$), and the energy spectrum curve slope showed an upward trend. The energy spectrum curve slope of common iliac vein was significantly different between

high expression and low expression of Ki67 ($P < 0.05$), and the slope of high expression of Ki67 was higher than that of low expression of Ki67 (Table 5 and Figure 3).

Changes in the energy spectrum curve slope before and after treatment

In this study, 17 participants were treated effectively and 11 were not treated. After treatment, the slope of cervix energy spectrum curve and common iliac vein energy spectrum curve in the effective group were significantly increased compared with before treatment ($P < 0.05$), while the slope of cervix energy spectrum curve in the ineffective group was increased compared with before treatment, but the difference was not significant ($P > 0.05$) (Table 6).

Pathological features were distinguished by different slope of energy spectrum curve

An ROC curve of cervical energy spectrum curve slope was constructed to distinguish pathological grade, and the results showed that the AUC was 0.8248 [95% confidence interval (CI): 0.7576 to 0.8921], with sensitivity of 81.25%, and specificity of 74.68% (Figure 4A). The ROC curve of energy spectrum curve slope of common iliac vein to distinguish the expression of Ki67 was constructed, and the results showed that the AUC was 0.7008 (95% CI: 0.6100 to 0.7915), the sensitivity and specificity were 66.67% and 62.34%, respectively (Figure 4B). The ROC curve of cervical energy spectrum curve slope to distinguish the curative effect was constructed, and the results showed that the AUC was 0.6131 (95% CI: 0.5194 to 0.7068),

Table 2 Relationship between CT value and pathological features of cervix

Single energy (cervix)	Squamous cell carcinoma	Adenocarcinoma	Squamous cell carcinoma with adenoid differentiation	Low differentiation	Middle differentiation	High differentiation	High expression of Ki67	Low expression of Ki67
40 keV	178.94±36.86	212.08±37.48	199.37±31.73	228.36±27.39	182.15±24.97*	188.66±22.38*	227.13±44.69	187.39±48.02 [#]
50 keV	130.44±22.76	152.61±25.12	143.51±53.82	161.42±19.35	131.92±18.97*	137.68±18.09*	161.41±28.91	136.64±30.56 [#]
60 keV	100.59±14.49	116.02±17.60	109.10±36.78	120.32±14.48	101.03±14.24	106.32±19.47	103.58±19.46	105.38±20.14
70 keV	82.03±9.79	93.27±13.06	87.78±26.31	94.28±11.62	81.79±9.69	86.82±14.19	83.79±13.88	85.97±13.95
80 keV	70.15±7.44	78.72±10.22	74.08±19.69	77.82±9.85	69.50±7.16	74.33±10.97	71.12±10.60	73.54±10.39
90 keV	62.29±6.46	69.08±8.43	65.07±15.47	66.92±8.77	61.34±5.84	66.08±8.94	62.73±8.74	65.32±8.42
100 keV	56.83±6.22	62.39±7.22	58.76±12.64	59.33±7.89	55.68±5.28	60.33±7.65	56.91±7.67	59.59±7.41
110 keV	56.83±6.17	57.66±6.45	54.32±10.74	54.00±7.42	51.72±5.10	56.28±6.83	52.80±7.14	55.56±6.95
120 keV	52.98±6.32	54.44±5.93	51.31±9.53	50.32±7.03	48.99±5.11	53.53±6.30	50.02±6.87	52.83±6.79
130 keV	50.37±6.50	51.82±5.58	48.83±8.63	47.40±6.78	46.76±5.17	51.28±5.94	47.72±6.72	50.57±6.76
140 keV	48.21±6.69	49.78±5.31	46.91±8.03	45.07±6.54	45.02±5.27	49.53±5.71	45.94±6.68	48.84±6.81

* , P<0.05 compared with low differentiation; [#] , P<0.05 compared with high expression of Ki67. CT, computed tomography; Ki67, cell proliferation antigen marker.

Table 3 Relationship between CT value and pathological characteristics of uterine body

Single energy (uterine body)	Squamous cell carcinoma	Adenocarcinoma	Squamous cell carcinoma with adenoid differentiation	Low differentiation	Middle differentiation	High differentiation	High expression of Ki67	Low expression of Ki67
40 keV	219.53±39.94	271.70±35.98 ^a	257.67±38.93	209.25±65.75	227.19±38.59	218.89±66.12	229.75±63.48	235.88±39.40
50 keV	156.76±22.54	192.20±23.48 ^a	175.74±26.11	151.23±43.78	160.97±24.34	157.23±45.03	162.45±41.03	168.30±26.69
60 keV	118.16±22.04	143.19±10.61	130.33±30.47	115.29±30.26	120.28±15.75	119.29±32.20	121.03±27.37	126.70±19.06
70 keV	94.16±15.71	112.88±9.59	100.13±21.52	93.11±21.89	94.97±10.66	95.71±24.38	95.31±19.04	100.88±14.63
80 keV	78.82±11.86	93.39±8.93	80.82±15.76	78.79±16.54	78.80±7.65	80.64±19.41	78.86±13.82	84.33±11.98
90 keV	68.64±9.53	80.59±8.62	68.10±12.03	68.55±13.08	68.06±6.03	70.67±16.22	67.96±10.56	73.40±10.44
100 keV	61.58±8.10	71.59±8.39	59.24±9.50	62.93±10.61	60.62±5.24	63.74±14.05	60.37±8.48	65.79±9.44
110 keV	56.61±7.27	65.26±8.19	52.98±7.79	58.21±8.79	55.39±4.88	58.81±12.65	55.07±7.23	60.41±8.82
120 keV	53.19±6.80	60.94±8.10	48.66±6.59	55.19±7.57	51.76±4.84	55.46±11.65	51.37±6.49	56.76±8.45
130 keV	50.45±6.49	54.47±8.09	45.23±5.68	52.59±6.64	48.88±4.85	52.82±10.91	48.42±6.02	53.83±8.18
140 keV	48.29±6.30	54.79±7.99	42.53±5.07	50.62±5.95	46.61±4.93	50.66±10.35	46.13±5.71	51.48±8.01

^a , P<0.05 compared with adenocarcinoma. CT, computed tomography; Ki67, cell proliferation antigen marker.

Table 4 Relationship between CT values and pathological features of common iliac vein

Single energy (common iliac vein)	Squamous cell carcinoma	Adenocarcinoma	Squamous cell carcinoma with adenoid differentiation	Low differentiation	Middle differentiation	High differentiation	High expression of Ki67	Low expression of Ki67
40 keV	303.74±57.76	327.79±48.83 ^a	330.68±51.79	398.05±43.70	292.62±47.15*	300.63±49.41*	304.88±55.37	320.36±56.94
50 keV	211.53±37.79	226.75±17.80	228.67±45.97	273.09±27.41	203.88±30.18	209.59±32.35	211.87±35.66	222.61±37.41
60 keV	154.85±25.69	164.64±11.68	165.95±30.18	196.29±13.61	149.31±20.04	153.64±21.98	154.74±23.67	162.48±25.59
70 keV	119.64±18.32	126.02±7.88	127.03±20.47	148.38±11.17	115.47±14.13	118.86±15.68	119.24±16.37	125.13±18.30
80 keV	97.05±13.82	101.28±5.50	102.08±14.42	117.78±9.82	93.70±10.71	96.59±11.78	96.48±11.86	101.18±13.89
90 keV	82.20±11.09	85.00±4.20	85.60±10.66	97.69±8.72	79.43±8.88	81.89±9.54	81.49±9.13	85.43±11.23
100 keV	71.84±9.33	73.75±3.32	74.15±8.28	73.71±7.84	69.46±7.90	71.72±8.06	71.08±7.39	74.46±9.43
110 keV	64.51±8.25	65.59±2.83	66.07±6.81	73.65±7.71	62.40±7.45	64.54±7.09	63.66±6.35	66.65±8.41
120 keV	59.44±7.57	60.07±2.58	60.39±6.01	66.71±7.11	57.53±7.25	59.45±6.58	57.54±5.76	61.20±7.70
130 keV	55.45±7.18	55.63±2.43	56.02±5.60	61.26±6.99	53.72±7.21	55.47±6.24	54.53±5.46	57.02±7.28
140 keV	52.31±6.90	52.24±2.46	52.55±5.39	57.08±6.82	50.66±7.22	52.42±6.01	51.36±5.27	53.72±7.01

* , P<0.05 compared with low differentiation; ^a , P<0.05 compared with adenocarcinoma. CT, computed tomography; Ki67, cell proliferation antigen marker.

with sensitivity and specificity of 56.25% and 59.09%, respectively (Figure 4C). The ROC curve of energy spectrum curve slope of common iliac vein to distinguish the curative effect was constructed, and the results showed that the AUC was 0.6563 (95% CI: 0.5464 to 0.7661), the sensitivity was 60.42%, and the specificity was 58.33% (Figure 4D).

Discussion

Cervical cancer is a common malignant tumor of the female reproductive system. The main pathological features include histological type, degree of differentiation, and expression of Ki67. The histological types of cervical cancer are mainly squamous cell carcinoma, adenocarcinoma, and squamous cell adenocarcinoma. Squamous cell carcinoma is the dominant type, accounting for about 90%, and adenocarcinoma accounts for 5%. At present, the use of efficient examination methods and early intervention treatment are helping to reduce the incidence of squamous cell carcinoma. However, because cervical adenocarcinoma is mostly endophytic, it is not easy to sample during cytological examination, resulting in a low detection rate of adenocarcinoma; therefore, the incidence of adenocarcinoma has gradually increased, and the age of onset has been decreasing (7). In a survey of the past 30 years, it was found that squamous cell carcinoma accounted for 70% and adenocarcinoma accounted for 20% (8). Squamous cell carcinoma and adenocarcinoma with the same International Federation of Gynecology and Obstetrics (FIGO) stage are treated in the same way, but it has been confirmed that the epidemiology, clinicopathological and molecular characteristics, treatment response, and prognosis of cervical squamous cell carcinoma and adenocarcinoma are different (9). The degree of pathological differentiation of cervical cancer can be divided into high differentiation, middle differentiation, low differentiation. The lower the degree of differentiation, the higher the heterogeneity, and the more prone to invasion and metastasis (10). Compared with tumors with low differentiation, tumors with high differentiation have better prognosis and lower recurrence rate. Existing studies have confirmed that low differentiation is an independent prognostic risk factor. The lower the degree of differentiation of cervical squamous cell carcinoma, the worse the prognosis. Patients with low-differentiation cervical cancer or histological type of adenocarcinoma have a significantly increased probability of metastasis after surgery, and the prognostic survival

Table 5 Relationship between the energy spectrum curve slope and the pathological characteristics

Energy spectrum curve slope (λ_{40-100})	Subtypes	Cervix	Uterine body	Common iliac vein
Pathological type	Squamous cell carcinoma	-1.14 ± 0.31	-1.45 ± 0.41	-2.05 ± 0.49
	Adenocarcinoma	-1.41 ± 0.28	-1.81 ± 0.93	-2.29 ± 0.23
	Squamous cell carcinoma with adenoid differentiation	-1.23 ± 0.53	-1.79 ± 0.54	-2.31 ± 0.59
	P value	0.2737	0.3100	0.4598
Differentiated degree	Low differentiation	-1.37 ± 0.06	-1.73 ± 0.11	-1.98 ± 0.26
	Middle differentiation	-1.12 ± 0.14	-1.63 ± 0.15	-1.91 ± 0.45
	High differentiation	-1.04 ± 0.04	-1.67 ± 0.13	-1.93 ± 0.20
	P value	0.0219	0.6064	0.9734
Ki67	High expression	-1.12 ± 0.35	-1.52 ± 0.33	-1.98 ± 0.38
	Low expression	-1.26 ± 0.43	-1.53 ± 0.58	-2.33 ± 0.51
	P value	0.3508	0.9543	0.0052

Ki67, cell proliferation antigen marker.

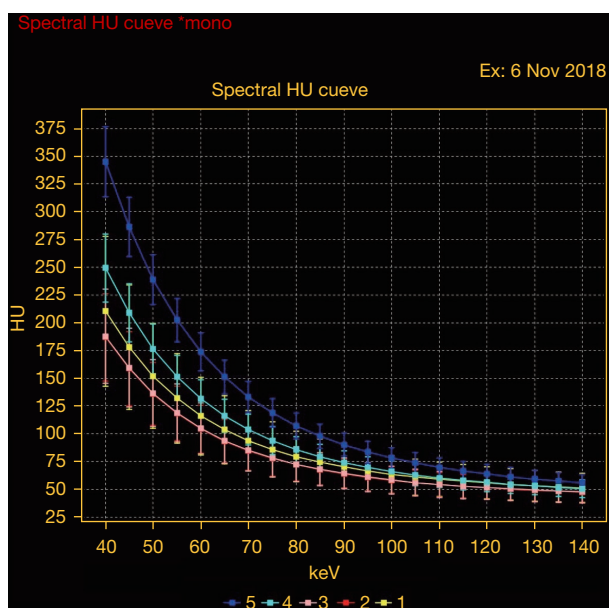


Figure 3 Energy spectrum curve of cervix, uterine body, and common iliac vein. The curves of each color represent the energy spectrum curves of each region of interest. No. 1-3 (yellow, red, pink) indicated cervical lesions. No. 4 (blue) indicated uterine body. No. 5 (dark blue) indicated common iliac vein. The curves represent the CT values of ROI under different KeV conditions. ROI, region of interest.

rate is reduced. The marker Ki67 is a prognostic marker of cancer, which is closely related to the proliferation, malignant degree, and prognosis of cervical tumor cells (11). Studies have shown that the prognosis of cervical cancer patients with high Ki67 expression was relatively poor (12). In clinical practice, due to the late stage of some cervical cancer patients, chemotherapy, targeted therapy, and other comprehensive treatment methods are chosen, so surgical pathology cannot be obtained, or puncture biopsy cannot be performed due to contraindications. Therefore, whether some pathological features and Ki67 expression can be assessed non-invasively before and after treatment is worthy of further study at this stage.

Clinically, magnetic resonance imaging (MRI) is often used to diagnose cervical cancer, while CT is often used in patients with intrauterine device (IUD) or contraindication to MRI. Traditional CT is mixed energy mode imaging, and the composition and properties of lesions are analyzed according to CT value, but the measurement of CT value can be changed due to X-ray hardening effect, power supply condition, scanning parameters and other factors, among which X-ray hardening effect is the main influencing factor (13). Energy spectrum CT can effectively overcome the X-ray hardening effect, and can reconstruct any single energy images of 40–140 keV. Each single energy level

Table 6 Changes in the energy spectrum curve slope before and after treatment

Energy spectrum curve slope (λ_{40-100})	Curative effect	Before treatment	After treatment	P value
Cervix	Effective (CR + PR)	-1.18±0.31	-0.85±0.29	0.0031
	Ineffective (SD + PD)	-1.11±0.46	-0.98±0.33	0.4552
Uterine body	Effective (CR + PR)	-1.60±0.29	-1.32±0.21	0.2785
	Ineffective (SD + PD)	-1.43±0.58	-1.46±0.47	0.8953
Common iliac vein	Effective (CR + PR)	-2.10±0.38	-1.79±0.31	0.0138
	Ineffective (SD + PD)	-2.16±0.54	-2.13±0.32	0.8756

CR, complete remission; PR, partial remission; SD, stable disease; PD, progressive disease.

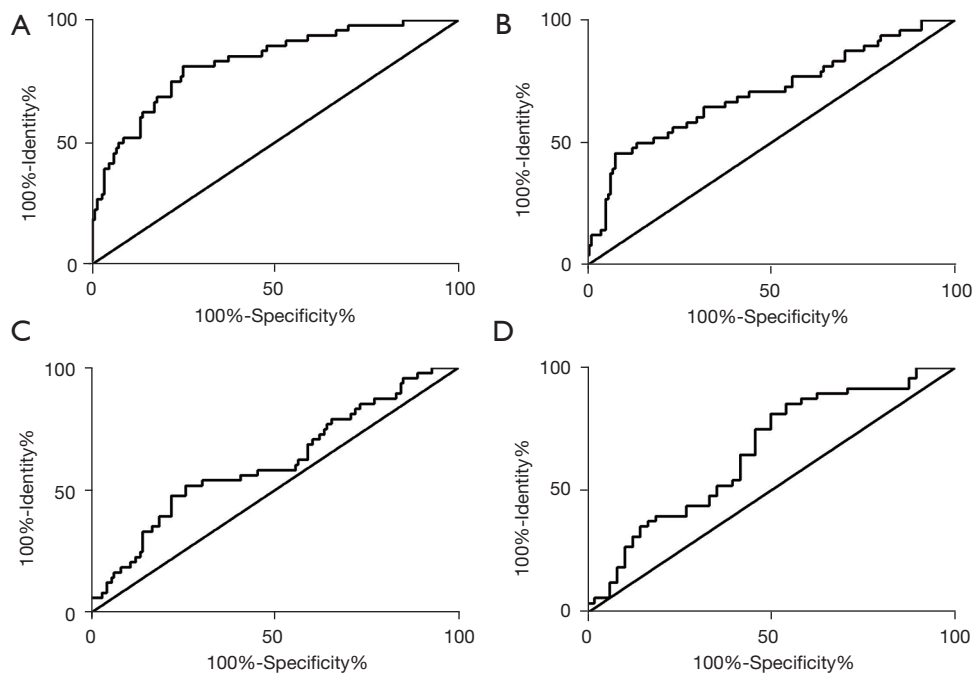


Figure 4 ROC curve. (A) ROC curve of cervical energy spectrum curve slope to distinguish pathological grade; (B) ROC curve of energy spectrum curve slope of common iliac vein to distinguish the expression of Ki67. (C) ROC curve of cervical energy spectrum curve slope to distinguish the curative effect. (D) ROC curve of energy spectrum curve slope of common iliac vein to distinguish the curative effect. ROC, receiver operating characteristic; Ki67, cell proliferation antigen marker.

corresponds to an accurate CT value, thus providing more accurate information than conventional CT mixed energy imaging, which is beneficial to the diagnosis of disease. Studies have confirmed that energy spectrum scanning mode can effectively reduce the influence of hardening artifacts on CT value, and obtain more accurate CT value than conventional scanning (14). In addition, energy spectrum CT provides a series of continuous energy images, from which the single energy image with best

contrast-to-noise ratio (CNR) can be selected to optimize the contrast between the lesion and the background and improve the discrimination of the lesion. Current research has found that images of 65 and 70 keV had lower noise and a higher CNR (15). The permeability of the new microvessels of the diseased mass is related to the CT value. Generally, malignant tumors have more blood vessels and higher permeability, so more contrast agents will diffuse into the cell space of malignant tumors during

enhanced scanning, resulting in a significant increase in CT value. Benign tumors generally lack blood vessels, and the diffusion of contrast agents in benign tumors is slow, resulting in a lower CT value than malignant tumors. Histologically, adenocarcinoma is prone to form abundant and uniform sieve-shaped capillaries, and there are more new blood vessels than squamous cell carcinoma. The more blood vessels supply the tumor, the greater the degree of enhancement, and the higher the iodine content of the tissue, which will cause more changes in the chemical composition and tissue metabolism in the lesion structure, thus leading to the morphological changes of the energy spectrum attenuation curve of the lesion. Generally, the slope of the energy spectrum curve will be relatively larger at this time (16).

In addition to the histological classification, there have been some reports on the relationship between the pathological grade, the expression of Ki-67, and the energy spectrum CT parameters. Lin *et al.* (17) showed that there was a significant negative correlation between energy spectrum CT parameters and pathological grade, and it had a certain ability to distinguish between high differentiation and low differentiation of tumors. Wang *et al.* (18) showed that in patients with esophageal squamous cell carcinoma, the slope of energy spectrum curve was positively correlated with Ki-67 expression at 40–80 keV.

The results of this study revealed that the cervical energy spectrum curve slope was significantly different in different degrees of differentiation ($P < 0.05$), the energy spectrum curve slope showed an upward trend, and the curve tended to be flat. The energy spectrum curve slope of the common iliac vein was significantly different between high and low Ki67 expression ($P < 0.05$), and the slope of high Ki67 expression was higher than that of low Ki67 expression. These results indicated that cervical cancer with different pathological features had different energy spectrum characteristics. After treatment, 17 participants with cervical cancer were treated effectively and the treatment of the remaining 11 was ineffective. The cervical energy spectrum curve slope and energy spectrum curve slope of common iliac vein in the effective group were significantly higher than before treatment ($P < 0.05$). It was inferred that after treatment, drugs destroyed tumor cells and enhanced anti-angiogenesis, resulting in decreased blood supply of lesions and decreased iodine intake, so that the energy spectrum curve of cancer foci tended to be flat. According to the significant difference of the energy spectrum curve slope among different pathological features, the respective

ROC curves were constructed. The results showed that the AUC of cervical energy spectrum curve slope to distinguish the degree of differentiation was 0.8248 (95% CI: 0.7756 to 0.8921), with sensitivity and specificity of 81.25% and 74.68%, respectively. The AUC of energy spectrum curve slope of common iliac vein to distinguish the expression of Ki67 was 0.7008 (95% CI: 0.6100 to 0.7915), with sensitivity and specificity of 66.67% and 62.34%, respectively. The AUC of cervical energy spectrum curve slope to distinguish the curative effect was 0.6131 (95% CI: 0.5194 to 0.7068), with sensitivity and specificity of 56.25% and 59.09%, respectively. The AUC of energy spectrum curve slope of common iliac vein to distinguish the curative effect was 0.6563 (95% CI: 0.5464 to 0.7661), with sensitivity and specificity of 60.42% and 58.33%, respectively. The above results indicated that the cervical energy spectrum curve slope had a high efficiency in distinguishing the degree of differentiation and had certain application value.

In conclusion, the energy spectrum curve slope has potential value for the prediction of certain pathological types of cervical cancer and the evaluation of curative effect.

Acknowledgments

Funding: None.

Footnote

Reporting Checklist: The authors have completed the STARD reporting checklist. Available at <https://dx.doi.org/10.21037/tcr-21-1320>

Data Sharing Statement: Available at <https://dx.doi.org/10.21037/tcr-21-1320>

Conflicts of Interest: All authors have completed the ICMJE uniform disclosure form (available at <https://dx.doi.org/10.21037/tcr-21-1320>). The authors have no conflicts of interest to declare.

Ethical Statement: The authors are accountable for all aspects of the work in ensuring that questions related to the accuracy or integrity of any part of the work are appropriately investigated and resolved. The study was conducted in accordance with the Declaration of Helsinki (as revised in 2013). All participants provided written informed consent, and this experiment was approved by the

Ethics Committee of Shaanxi Provincial Cancer Hospital (202061684).

Open Access Statement: This is an Open Access article distributed in accordance with the Creative Commons Attribution-NonCommercial-NoDerivs 4.0 International License (CC BY-NC-ND 4.0), which permits the non-commercial replication and distribution of the article with the strict proviso that no changes or edits are made and the original work is properly cited (including links to both the formal publication through the relevant DOI and the license). See: <https://creativecommons.org/licenses/by-nc-nd/4.0/>.

References

1. Olusola P, Banerjee HN, Phillely JV, et al. Human Papilloma Virus-Associated Cervical Cancer and Health Disparities. *Cells* 2019;8:622.
2. Zhang X, Guo J, Cai Y, et al. Whole-exome sequencing in cervical adenocarcinoma in mainland Chinese patients. *Transl Cancer Res* 2020;9:6889-99.
3. Hurrell MA, Butler AP, Cook NJ, et al. Spectral Hounsfield units: a new radiological concept. *Eur Radiol* 2012;22:1008-13.
4. Tang L, Zhang XP, Sun YS, et al. Spectral CT in the demonstration of the gastrocolic ligament: a comparison study. *Surg Radiol Anat* 2013;35:539-45.
5. Li XH, Zhao R, Liu B, et al. Determination of urinary stone composition using dual-energy spectral CT: initial in vitro analysis. *Clin Radiol* 2013;68:e370-7.
6. Ma T, Cao LX, Li HJ, et al. Different Energy Spectrum CT Findings between Anterior Mediastinal Lymphoma and Thymic Carcinoma. *Zhongguo Yi Xue Ke Xue Yuan Xue Bao* 2020;42:431-5.
7. Wang SS, Carreon JD, Gomez SL, et al. Cervical cancer incidence among 6 asian ethnic groups in the United States, 1996 through 2004. *Cancer* 2010;116:949-56.
8. Li S, Hu T, Lv W, et al. Changes in prevalence and clinical characteristics of cervical cancer in the People's Republic of China: a study of 10,012 cases from a nationwide working group. *Oncologist* 2013;18:1101-7.
9. Fujiwara K, Monk B, Devouassoux-Shisheboran M. Adenocarcinoma of the uterine cervix: why is it different? *Curr Oncol Rep* 2014;16:416.
10. Li Y, Liu K, Ke Y, et al. Risk Factors Analysis of Pathologically Confirmed Cervical Lymph Nodes Metastasis in Oral Squamous Cell Carcinoma Patients with Clinically Negative Cervical Lymph Node: Results from a Cancer Center of Central China. *J Cancer* 2019;10:3062-9.
11. Gothwal M, Nalwa A, Singh P, et al. Role of Cervical Cancer Biomarkers p16 and Ki67 in Abnormal Cervical Cytological Smear. *J Obstet Gynaecol India* 2021;71:72-7.
12. Silva DC, Gonçalves AK, Cobucci RN, et al. Immunohistochemical expression of p16, Ki-67 and p53 in cervical lesions - A systematic review. *Pathol Res Pract* 2017;213:723-9.
13. Machida H, Tanaka I, Fukui R, et al. Dual-Energy Spectral CT: Various Clinical Vascular Applications. *Radiographics* 2016;36:1215-32.
14. Goo HW, Goo JM. Dual-Energy CT: New Horizon in Medical Imaging. *Korean J Radiol* 2017;18:555-69.
15. Punjabi GV. Multi-energy spectral CT: adding value in emergency body imaging. *Emerg Radiol* 2018;25:197-204.
16. Zhang G, Cao Y, Zhang J, et al. Epidermal growth factor receptor mutations in lung adenocarcinoma: associations between dual-energy spectral CT measurements and histologic results. *J Cancer Res Clin Oncol* 2021;147:1169-78.
17. Lin LY, Zhang Y, Suo ST, et al. Correlation between dual-energy spectral CT imaging parameters and pathological grades of non-small cell lung cancer. *Clin Radiol* 2018;73:412.e1-7.
18. Wang P, Tang Z, Xiao Z, et al. Dual-energy CT in predicting Ki-67 expression in laryngeal squamous cell carcinoma. *Eur J Radiol* 2021;140:109774.

(English Language Editor: J. Jones)

Cite this article as: Pan L, Jia X, Zhao X, Zhang B, Wang S, Fan T, Zhou M, Yuan Y, Wang G, Xue L. Study on the correlation between energy spectrum computed tomography imaging and the pathological characteristics and prognosis of cervical cancer. *Transl Cancer Res* 2021;10(9):4096-4105. doi: 10.21037/tcr-21-1320